EXTENDED PDF FORMAT
SPONSORED BY
BIO-RAD
http://discover.bio-rad.com

Pairing Without Superfluidity: The Ground State of an Imbalanced Fermi Mixture

C. H. Schunck, *et al.*

Science **316**, 867 (2007);
DOI: 10.1126/science.1140749

The following resources related to this article are available online at www.sciencemag.org (this information is current as of May 10, 2007):

Updated information and services, including high-resolution figures, can be found in the online version of this article at:
http://www.sciencemag.org/cgi/content/full/316/5826/867

Supporting Online Material can be found at:
http://www.sciencemag.org/cgi/content/full/316/5826/867/DC1

This article **cites 30 articles**, 4 of which can be accessed for free:
http://www.sciencemag.org/cgi/content/full/316/5826/867#otherarticles

This article appears in the following **subject collections**:
Physics
http://www.sciencemag.org/cgi/collection/physics

Information about obtaining **reprints** of this article or about obtaining **permission to reproduce this article** in whole or in part can be found at:
http://www.sciencemag.org/about/permissions.dtl

Downloaded from www.sciencemag.org on May 10, 2007

Science (print ISSN 0036-8075; online ISSN 1095-9203) is published weekly, except the last week in December, by the American Association for the Advancement of Science, 1200 New York Avenue NW, Washington, DC 20005. Copyright c 2007 by the American Association for the Advancement of Science; all rights reserved. The title SCIENCE is a registered trademark of AAAS.

Pairing Without Superfluidity: The Ground State of an Imbalanced Fermi Mixture

C. H. Schunck,* Y. Shin, A. Schirotzek, M. W. Zwierlein,† W. Ketterle

We used radio-frequency spectroscopy to study pairing in the normal and superfluid phases of a strongly interacting Fermi gas with imbalanced spin populations. At high spin imbalances, the system does not become superfluid even at zero temperature. In this normal phase, full pairing of the minority atoms was observed. Hence, mismatched Fermi surfaces do not prevent pairing but can quench the superfluid state, thus realizing a system of fermion pairs that do not condense even at the lowest temperature.

Fermionic superfluidity has many manifestations in nature; it occurs in such diverse systems as superconducting materials, liquid ^{3}He, neutron stars, and ultracold quantum gases. At its heart lies the formation of fermion pairs. Although the Pauli principle forbids identical fermions to occupy the same quantum state, pairs of fermions can condense and thus become superfluid. Superconductivity, the flow of electrical current without resistance, is a manifestation of fermionic superfluidity in a condensed-matter system. Superconductors are characterized by a temperature T^* where electrons start to pair and a critical temperature T_c for the onset of superconductivity. In conventional superconductors, understood within the framework of Bardeen-Cooper-Schrieffer (BCS) theory, fermion pairs form and condense simultaneously (i.e., $T^* = T_c$). In high-temperature superconductors, strongly correlated electrons exist in the normal phase, that is, $T^* > T_c$. The interactions that mediate pairing and ultimately lead to superconductivity in these complex systems are still subject to debate (*1*). Another strongly interacting but comparatively simple fermion system is an ultracold gas of neutral fermionic atoms. High-temperature superfluidity was recently observed in these gases (*2*), opening a new approach to explore the highly correlated normal phase of strongly interacting fermions and its relation to the onset of superfluidity.

Ultracold atomic Fermi mixtures of two spin states close to a Feshbach resonance constitute a highly controllable model system for strongly interacting fermions. By resonantly changing the interaction strength between the fermionic atoms, the crossover from BCS superfluidity of loosely bound pairs to Bose-Einstein condensation (BEC) of tightly bound molecules can be explored. BEC-BCS crossover theory at finite temperature contains pairing in the normal phase below a temperature $T^* > T_c$ (*1*, *3*–*5*). Evidence for pairing above T_c in ultracold Fermi gases was found in (*6*, *7*) via radio-frequency (rf) spectroscopy. Here, we use rf spectroscopy to study primarily the normal state of an imbalanced spin mixture. An imbalance in the spin populations of the two-state Fermi system leads to a qualitative change of the phase diagram: Above a certain interaction-dependent population imbalance, the transition to the superfluid state is suppressed even at zero temperature. This is known as the Chandrasekhar-Clogston (CC) or Pauli paramagnetic limit of superfluidity (*8*, *9*). In several works, the CC limit is assumed to imply pair dissociation and is referred to as "Pauli pair breaking" (*10*–*12*), that is, T^* and T_c are assumed to vanish simultaneously. The CC limit has been observed and characterized in ultracold atomic gases (*13*).

We report on the observation of a gap in a single-particle excitation spectrum (representing a spin response function) of a highly imbalanced sample. This implies that the system is in a correlated state and that the minority component is paired. Pairing of fermions is thus not necessarily a precursor to superfluidity: T^* is finite even when T_c vanishes. The CC limit of superfluidity, at least for strong interactions, is not associated with breaking of fermion pairs but only with the quenching of the superfluid state. Another and probably very different system with finite T^* and vanishing T_c has been discussed in strongly underdoped cuprates (*1*).

The rf spectra presented in this work were also correlated with an indirect signature for superfluidity by determining pair condensate fractions (*14*, *15*). We conclude that rf spectra cannot distinguish, at present experimental resolution, between normal and superfluid states.

In our experiment, a strongly interacting, imbalanced spin mixture of ^{6}Li fermions in the two lowest hyperfine states, labeled $|1\rangle$ and $|2\rangle$ (corresponding to the $|F = {}^1\!/_2, m_F = {}^1\!/_2\rangle$ and $|F = {}^1\!/_2, m_F = -{}^1\!/_2\rangle$ states at low magnetic field) was created in an optical dipole trap at 833 G, the center of the $|1\rangle$-$|2\rangle$ Feshbach resonance [see (*15*, *16*) for details]. On resonance, all interactions in the $|1\rangle$-$|2\rangle$ mixture are universal, as the Fermi energy E_F and the inverse Fermi wavenumber $1/k_F$ are the only relevant energy and length scales. The imbalance δ of the mixture was controlled as reported in (*13*, *17*), where $\delta = (N_1 - N_2)/(N_1 + N_2)$ and N_1 and N_2 are the atom numbers in states $|1\rangle$ and $|2\rangle$, respectively. Here, E_F, k_F, and the Fermi temperature T_F are given for a noninteracting Fermi gas with the same atom number as the majority component. To access a broader range of temperatures, we used two optical traps with different waists, characterized by the axial and radial trapping frequencies ω_a and ω_r (as given in the figure captions of the rf spectra).

The interactions were spectroscopically probed in a three-level system (*18*). A 2-ms rf pulse resonant with the transition from state $|2\rangle$ (the minority component) to a third state, labeled $|3\rangle$ ($|F = {}^3\!/_2, m_F = -{}^3\!/_2\rangle$ at low field) was applied. Immediately after the rf pulse, the optical trap was switched off and the cloud was allowed to expand for absorption imaging. Two absorption images of atoms in states $|2\rangle$ and $|1\rangle$ were taken successively, and the atom number fraction $N_2/(N_1 + N_2)$ was obtained as a function of the applied rf. The rf spectra at the highest imbalances were taken with a population transfer smaller than 3% of the total number of atoms. The data points in all spectra are the average of three

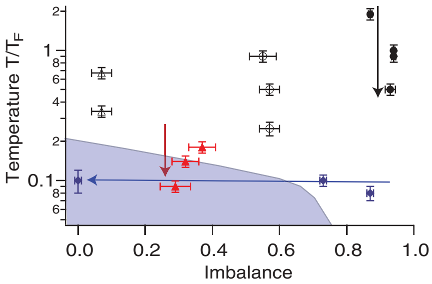

Fig. 1. The temperature-imbalance diagram shows where the rf spectra presented in Fig. 2 (black circles), Fig. 4, A to C (blue diamonds), and Fig. 4, D to F (red triangles) were taken. All spectra were obtained on resonance at 833 G. The arrows indicate the order in which the spectra are displayed in the figures. The shaded region indicates the superfluid phase. The spectra corresponding to the open circles and triangles are similar to the spectra of Fig. 2, A to C, and are shown in (*19*). Except for the data close to zero imbalance, for which the interacting temperature T' is given, temperatures have been determined from the noninteracting wings of the majority cloud (*25*).

Department of Physics, MIT-Harvard Center for Ultracold Atoms, and Research Laboratory of Electronics, Massachusetts Institute of Technology, Cambridge, MA 02139, USA.

*To whom correspondence should be addressed. E-mail: chs@mit.edu

†Present address: Institut für Physik, AG Quantum, Staudinger Weg 7, 55128 Mainz, Germany.

independent measurements. Temperature was adjusted by evaporation to different depths of the optical trap, followed by recompression. Spectra presented as a data set were taken with the same final trap depth. Figure 1 provides an overview of the imbalances and temperatures at which the rf spectra were obtained. Specific details are given in the figure captions and in (*19*). All radio frequencies were referenced to the $|2\rangle$-$|3\rangle$ resonance recorded in the absence of atoms in state $|1\rangle$.

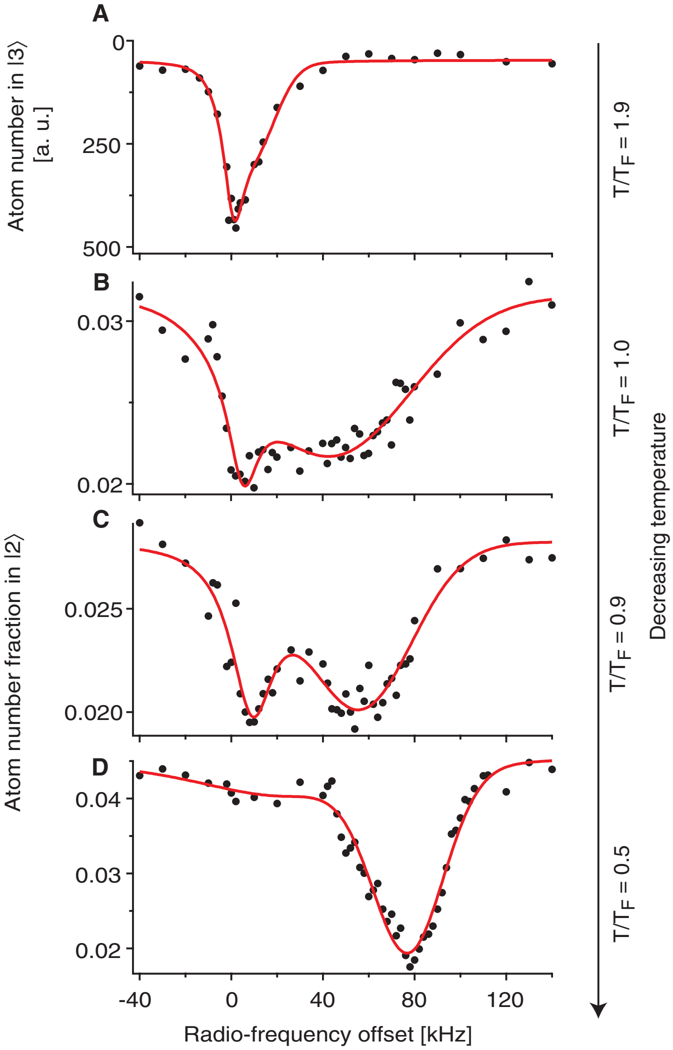

Fig. 2. Radio-frequency spectroscopy of the minority component in an imbalanced ($\delta \sim 0.9$), strongly interacting mixture of fermionic atoms above the CC limit of superfluidity. As the temperature is lowered, full pairing develops in the absence of superfluidity. (**A**) An asymmetric and broad peak centered at the position of the atomic line is observed. The asymmetry and the large width might be caused by the presence of pairing correlations already at $T/T_F = 1.9$. For this spectrum only, heating was applied and the atom number in state $|3\rangle$ was recorded (*19*). (**B** and **C**) The pairing peak emerges. (**D**) At $T/T_F = 0.5$, the pairing peak remains and the minority atoms are almost fully paired (see also Fig. 4A). As a guide to the eye, a double-peak line consisting of a Lorentzian fit to the atomic peak and a Gaussian fit to the pairing peak is included. Spectra were taken for the following parameters (see also the solid black circles in Fig. 1): (A) $\delta = 0.87$, $E_F = h \times 260$ kHz, $T/T_F = 1.9$; (B) $\delta = 0.94$, $E_F = h \times 360$ kHz, $T/T_F = 1.0$; (C) $\delta = 0.94$, $E_F = h \times 360$ kHz, $T/T_F = 0.9$; (D) $\delta = 0.93$, $E_F = h \times 340$ kHz, $T/T_F = 0.5$. The trapping frequencies were $\omega_r = 2\pi \times 3.5$ kHz and $\omega_a = 2\pi \times 77$ Hz.

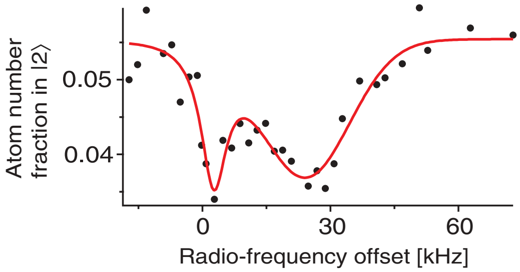

Fig. 3. Radio-frequency spectrum of the minority component obtained at a magnetic field of 937 G ($1/k_F a_{12} = -0.18$) and imbalance $\delta = 0.88$, demonstrating strong pairing above the CC limit on the BCS side of the Feshbach resonance (a_{12} is the s-wave scattering length in the $|1\rangle$-$|2\rangle$ mixture). The rf spectrum was taken for the parameters $E_F = h \times 280$ kHz and $T/T_F = 0.3$. The trapping frequencies were $\omega_r = 2\pi \times 2.9$ kHz and $\omega_a = 2\pi \times 64$ Hz.

The rf spectroscopy measures a single-particle spin excitation spectrum for the minority component of the mixture (*20–23*). To understand the expected rf spectra, one can use a simplified description of the gas as a mixture of free atoms and molecule-like pairs, which is strictly valid only in the BEC limit. Transferring an unbound atom from state $|2\rangle$ into state $|3\rangle$ requires an energy ΔE_{23}. As the $|1\rangle$-$|3\rangle$ mixture is also strongly interacting because of a $|1\rangle$-$|3\rangle$ Feshbach resonance located at 690 G (*18*), we first assume, as in (*6*, *7*), that mean-field shifts (i.e., shifts corresponding to Hartree terms) are absent in the rf spectrum. Then ΔE_{23} and the width of the atomic $|2\rangle$-$|3\rangle$ transition are independent of the density of atoms in state $|1\rangle$. However, if an atom in state $|2\rangle$ is paired with an atom in state $|1\rangle$, the rf photon must provide the binding energy E_B required to break the pair in addition to ΔE_{23}. Therefore, if pairing is present in the system, a second peak emerges in the minority rf spectrum that is separated from the atomic line and associated with pairing (*6*, *7*). In a Fermi cloud, pairing is strong only near the Fermi surface. Because the rf photons can excite atoms in the whole Fermi sea, the observed spectral gap $\Delta\nu$ may have to be interpreted as a pair-binding energy averaged over the Fermi sea. Indeed, in the BCS limit one has $h\Delta\nu \propto \Delta^2/E_F$, where h is Planck's constant and Δ is the BCS pairing gap (*23*). Under these working assumptions, we interpret the emergence of a gap in the spectrum as a pairing effect.

The presence of pairing in the normal phase has been observed in the rf spectra for a highly imbalanced mixture, with $\delta \sim 0.9$, on resonance at 833 G (Fig. 2) and on the BCS side at 937 G (Fig. 3). At high temperature, only the atomic peak was present, and as the temperature was lowered, a second peak—the pairing peak—emerged and separated from the atomic peak. At sufficiently low temperatures, essentially only the pairing peak remained. This behavior is qualitatively similar to what has been observed in an equal mixture (*6*). The spectral gap $\Delta\nu$ (i.e., the shift of the pairing peak relative to the atomic line) increases as the temperature is lowered. At the lowest temperature of $0.08T/T_F$ (Fig. 4A), we measured a shift of $0.38E_F$.

All the spectra in Figs. 2 and 3 were obtained at high imbalances above the CC limit of superfluidity. Here the system cannot undergo a phase transition to the superfluid state even at zero temperature. For a trapped gas on resonance the CC limit is reached at a critical imbalance of $\delta_{c,\mathrm{exp}} = 0.74 \pm 0.05$ (*13*, *17*), in agreement with a calculated value of $\delta_{c,\mathrm{theory}} = 0.77$ (*24*). On the BCS side of the Feshbach resonance, at an interaction strength of $1/k_F a_{12} = -0.18$, the critical imbalance is $\delta_{c,\mathrm{exp}} = 0.6 \pm 0.1$, as previously measured around this interaction strength (*13*).

Because we observed full pairing in the normal phase of the strongly interacting gas, one might not expect the rf spectra to reveal the onset of superfluidity. We recorded rf spectra covering the phase transition from the normal to the superfluid state by varying imbalance (Fig. 4, A to C) as well as temperature (Fig. 4, D to F). In both cases, no signature of the phase transition was resolved, although both the emergence of fermion pair condensates and sudden changes in the density profiles (*13*, *17*) showed the phase transition. In our previous work (*2*, *13*), these indirect indicators of superfluidity were correlated with the presence of quantized vortices (i.e., superfluid flow).

Figure 4, A to C, illustrates that working with high imbalances has the advantage of reducing line-broadening effects that arise from averaging over the inhomogeneous density distribution of the sample. The narrowest line was observed at the highest imbalance (Fig. 4A), where the minority is considerably smaller than the majority cloud. The homogeneous linewidth should reflect the wave function of a single fermion pair. The observed narrow linewidth indicates localization in momentum space well below the Fermi momentum k_F, and hence a pair size on the order of the interparticle spacing.

We now examine the assumptions underlying our interpretation of the peaks in the rf spectra. In particular, we address the question of whether our observations can distinguish between pairing correlations and mean-field effects. Indeed, mean-field–like shifts were observed, for example, in the rf spectrum of Fig. 2C where the atomic line shows a shift of $0.03E_F$ to higher energy. Although the $|1\rangle$-$|3\rangle$ interactions are in the unitary regime for a typical value of $k_Fa_{13} \approx -3.3$ (varying, for example, from –3 to –3.6 across the minority cloud in Fig. 2C), they may not have fully converged to their value at unitarity and thus may have caused the observed shifts (a_{13} is the *s*-wave scattering length in the $|1\rangle$-$|3\rangle$ mixture). However, all shifts of the atomic line are small relative to the size of the spectral gap of up to $0.38E_F$ and are only seen in the presence of the pairing peak (fig. S3 displays all observed shifts of atomic and pairing peaks versus temperature). Although the shifts of the atomic line are small at all temperatures, the shifts associated with the pairing peak start rising below $T/T_F \sim 1$, accompanied by a decrease in the weight of the atomic line. In the intermediate temperature range, where the rf spectra show a double-peak structure, the pairing peak should originate primarily from the higher-density region in the center of the cloud, and the atomic peak should originate from the low-density wings. Therefore, if one were to normalize the data according to the local density of majority atoms, the data points for the atom peaks would shift up in T/T_F by a factor of between 1.5 and 5, the smaller factor reflecting the cases of large imbalance, where the minority cloud is considerably smaller than the majority cloud. As a result, near $T/T_{F(local)} = 0.5$, we have observed both atomic peaks and pairing peaks, which is an indication for the local coexistence of unpaired and paired minority atoms. However, in this possible coexistence region, either the peak separation is small or one peak has very small weight. Therefore, more work is needed to study the possibility of coexistence. An alternative interpretation assumes single local peaks and a sudden onset of peak shifts below $T/T_F \sim 1$. This appears to be incompatible with a local mean-field approximation as well: The mean field in the unitarity limit should saturate when T approaches T_F and not vary strongly for $T < T_F$, because the relative momentum of two particles in this regime is dominated by the Fermi momentum and not by the thermal

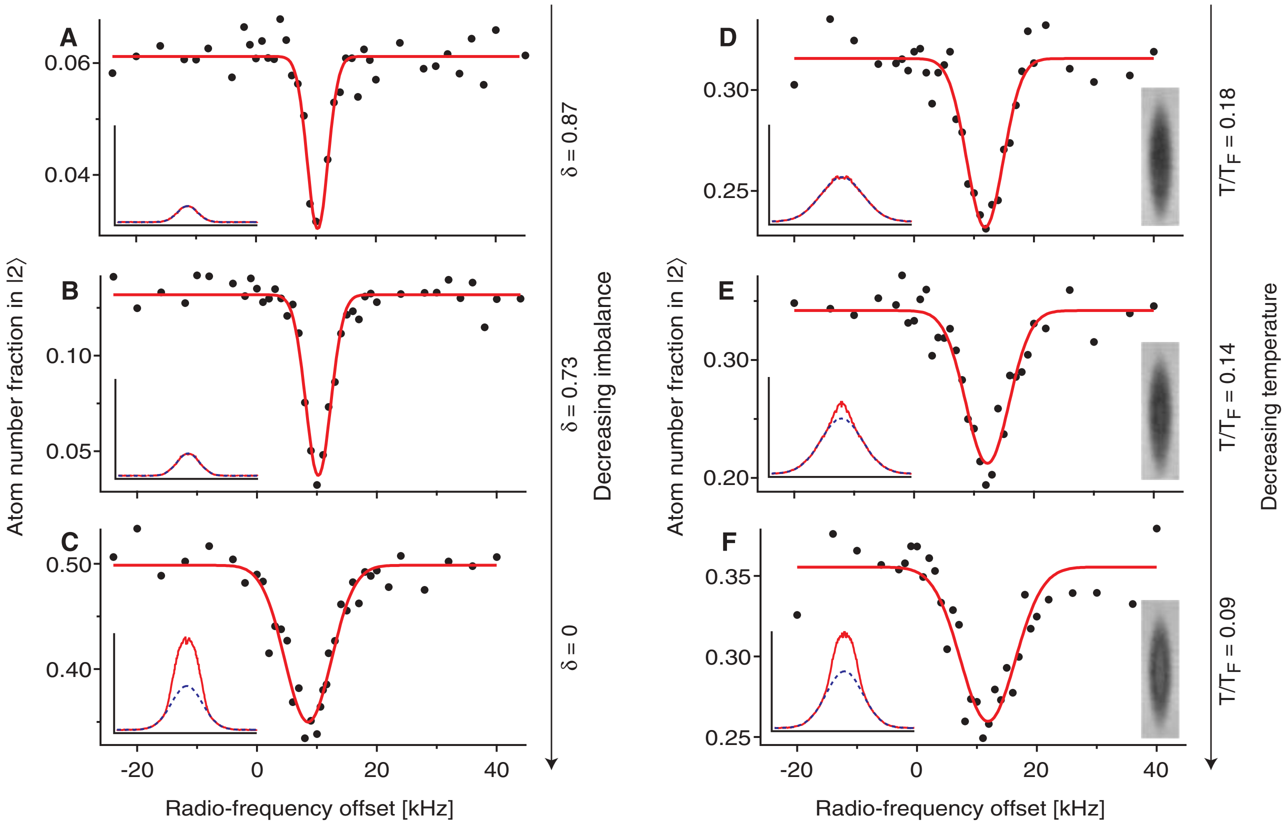

Fig. 4. Radio-frequency spectra of the minority component obtained while crossing the phase transition by reducing imbalance (**A** to **C**) and temperature (**D** to **F**). The rf spectra do not reveal the phase transition. The onset of superfluidity is indirectly observed by fermion pair condensation. The condensate fractions are zero in (A) and (B) and 35 ± 2% in (C). The onset of superfluidity as a function of temperature occurs between (D) and (F), with condensate fractions of 0% in (D), 3 ± 2% in (E), and 17 ± 3% in (F). The insets in (A) to (F) show the column density profile (red) of the minority cloud after a rapid magnetic field ramp to the BEC side and further expansion (*19*); the blue dashed line is a Gaussian fit to the thermal background. The additional insets in (D) to (F) show phase-contrast images for a trapped cloud, obtained at imbalances of the opposite sign. Spectra were taken for the following parameters in (A) to (C) (see also the blue diamonds in Fig. 1): (A) $\delta = 0.87$, $E_F = h \times 27$ kHz, $T/T_F = 0.08$; (B) $\delta = 0.73$, $E_F = h \times 27$ kHz, $T/T_F = 0.10$; (C) $\delta = 0.00$, $E_F = h \times 23$ kHz, $T'/T_F = 0.10$. The trapping frequencies were $\omega_r = 2\pi \times 143$ Hz and $\omega_a = 2\pi \times 23$ Hz. For the spectrum in (C) we quote the temperature T' obtained from a fit to the interacting Fermi gas (*19*). Spectra were taken for the following parameters in (D) to (F) (see also the solid red triangles in Fig. 1): (D) $\delta = 0.37$, $E_F = h \times 38$ kHz, $T/T_F = 0.18$; (E) $\delta = 0.32$, $E_F = h \times 38$ kHz, $T/T_F = 0.14$; (F) $\delta = 0.29$, $E_F = h \times 35$ kHz, $T/T_F = 0.09$. The trapping frequencies were $\omega_r = 2\pi \times 192$ Hz and $\omega_a = 2\pi \times 23$ Hz.

momentum. Furthermore, a sudden onset of interactions would likely affect the density distribution of the minority atoms. However, the minority clouds observed in expansion are well fit by a single Thomas-Fermi profile (*25*).

The BEC-side picture of a mixture of single atoms and molecules seems to extend into the resonance region, in the sense that fermion pairs form high above the superfluid transition temperature and possibly coexist locally with unpaired atoms. However, the fermion pairs on resonance behave differently from "real" molecules: Their binding energy increases with lower temperature and higher atomic density. Most important, fermion pairs above the CC limit do not condense at low temperature as bosonic molecules would do at any imbalance. Although some extensions of BCS mean-field theories to the imbalanced case do not predict pairing at imbalances δ above the CC limit (*26*), a survival of Cooper pairs "far from the transition region" has been predicted (*27*) for a superconducting system that is driven into the normal, paramagnetic phase by Zeeman splitting.

The observed spectral gaps appear to be insensitive to the density of the minority atoms (Fig. 4, A to C). At very high imbalances, one should indeed approach the limit of one minority atom immersed in a fully polarized Fermi sea. In (*24*, *28*, *29*) the ground-state energy for this scenario has been calculated to be about $-0.6E_F$, for example, by using a modified Cooper-pair wave function ansatz (*28*). These calculations do not provide an excitation spectrum and do not distinguish between pairing (correlation) energies and mean-field (Hartree) terms. Therefore, the theoretical result cannot be directly compared to our spectroscopic measurement of $h\Delta\nu = -0.38E_F$ at $T/T_F = 0.08$.

Whether superfluidity can occur for large imbalances and low atom numbers in highly elongated geometries remains a subject of debate (*30*). In light of our findings, it may be important to clearly distinguish between the effects of pairing and of superfluidity. It has also been suggested that the presence of an atomic peak next to the pairing peak in the minority cloud at zero temperature and high imbalance could provide evidence for exotic forms of superfluidity, such as the Fulde-Ferrel-Larkin-Ovchinnikov state (*31*). However, for the parameters studied here, the atomic peak is seen to disappear as the temperature is reduced (Figs. 2 and 4A).

Working with imbalanced Fermi gases, we were able to study and characterize pairing in a situation where no superfluidity occurs even at zero temperature. The spectral gap $\Delta\nu$ appears to be only weakly dependent on the imbalance. This finding suggests that near unitarity, certain pairing correlations in the superfluid state are similar to those in a dilute cloud of minority atoms immersed into the Fermi sea of the majority. Moreover, it implies that the energetics that drive the normal-to-superfluid phase transition involve more than the observed pairing energy. Further studies of the strongly correlated normal state might yield new insights into the microscopic physics of the superfluid state.

References and Notes

1. P. A. Lee, N. Nagaosa, X.-G. Wen, *Rev. Mod. Phys.* **78**, 17 (2006).
2. M. W. Zwierlein, J. R. Abo-Shaeer, A. Schirotzek, C. H. Schunck, W. Ketterle, *Nature* **435**, 1047 (2005).
3. N. Trivedi, M. Randeria, *Phys. Rev. Lett.* **75**, 312 (1995).
4. A. Perali, P. Pieri, G. C. Strinati, C. Castellani, *Phys. Rev. B* **66**, 024510 (2002).
5. Q. Chen, J. Stajic, S. Tan, K. Levin, *Phys. Rep.* **412**, 1 (2005).
6. C. Chin *et al.*, *Science* **305**, 1128 (2004); published online 22 July 2004 (10.1126/science.1100818).
7. J. Kinnunen, M. Rodríguez, P. Törmä, *Science* **305**, 1131 (2004); published online 22 July 2004 (10.1126/science.1100782).
8. B. S. Chandrasekhar, *Appl. Phys. Lett.* **1**, 7 (1962).
9. A. M. Clogston, *Phys. Rev. Lett.* **9**, 266 (1962).
10. K. Capelle, *Phys. Rev. B* **65**, 100515 (2002).
11. M. Maśka, *Phys. Rev. B* **66**, 054533 (2002).
12. K. Kumagai *et al.*, *Phys. Rev. Lett.* **97**, 227002 (2006).
13. M. W. Zwierlein, A. Schirotzek, C. H. Schunck, W. Ketterle, *Science* **311**, 492 (2006); published online 21 December 2005 (10.1126/science.1122318).
14. C. A. Regal, M. Greiner, D. S. Jin, *Phys. Rev. Lett.* **92**, 040403 (2004).
15. M. W. Zwierlein *et al.*, *Phys. Rev. Lett.* **92**, 120403 (2004).
16. Z. Hadzibabic *et al.*, *Phys. Rev. Lett.* **91**, 160401 (2003).
17. Y. Shin, M. W. Zwierlein, C. H. Schunck, A. Schirotzek, W. Ketterle, *Phys. Rev. Lett.* **97**, 030401 (2006).
18. S. Gupta *et al.*, *Science* **300**, 1723 (2003); published online 8 May 2003 (10.1126/science.1085335).
19. See supporting material on *Science* Online.
20. J. Kinnunen, M. Rodríguez, P. Törmä, *Phys. Rev. Lett.* **92**, 230403 (2004).
21. Y. Ohashi, A. Griffin, *Phys. Rev. A* **72**, 063606 (2005).
22. Y. He, Q. Chen, K. Levin, *Phys. Rev. A* **72**, 011602 (2005).
23. Z. Yu, G. Baym, *Phys. Rev. A* **73**, 063601 (2006).
24. C. Lobo, A. Recati, S. Giorgini, S. Stringari, *Phys. Rev. Lett.* **97**, 200403 (2006).
25. M. W. Zwierlein, C. H. Schunck, A. Schirotzek, W. Ketterle, *Nature* **442**, 54 (2006).
26. C. Chien, Q. Chen, Y. He, K. Levin, *Phys. Rev. Lett.* **98**, 110404 (2007).
27. I. L. Aleiner, B. L. Altshuler, *Phys. Rev. Lett.* **79**, 4242 (1997).
28. F. Chevy, *Phys. Rev. A* **74**, 063628 (2006).
29. A. Bulgac, M. M. Forbes, *Phys. Rev. A* **75**, 031605(R) (2007).
30. G. B. Partridge *et al.*, *Phys. Rev. Lett.* **97**, 190407 (2006).
31. J. Kinnunen, L. M. Jensen, P. Törmä, *Phys. Rev. Lett.* **96**, 110403 (2006).
32. We thank W. Zwerger, P. Lee, K. Levin, and Q. Chen for stimulating discussions and D. Miller for critical reading of the manuscript. Supported by NSF and the Office of Naval Research.

Supporting Online Material

www.sciencemag.org/cgi/content/full/316/5826/867/DC1
Materials and Methods
Figs. S1 to S3
References

2 February 2007; accepted 29 March 2007
10.1126/science.1140749

The Process of Tholin Formation in Titan's Upper Atmosphere

J. H. Waite Jr.,[1]* D. T. Young,[1] T. E. Cravens,[2] A. J. Coates,[3] F. J. Crary,[1] B. Magee,[1]* J. Westlake[4]

Titan's lower atmosphere has long been known to harbor organic aerosols (tholins) presumed to have been formed from simple molecules, such as methane and nitrogen (CH_4 and N_2). Up to now, it has been assumed that tholins were formed at altitudes of several hundred kilometers by processes as yet unobserved. Using measurements from a combination of mass/charge and energy/charge spectrometers on the Cassini spacecraft, we have obtained evidence for tholin formation at high altitudes (~1000 kilometers) in Titan's atmosphere. The observed chemical mix strongly implies a series of chemical reactions and physical processes that lead from simple molecules (CH_4 and N_2) to larger, more complex molecules (80 to 350 daltons) to negatively charged massive molecules (~8000 daltons), which we identify as tholins. That the process involves massive negatively charged molecules and aerosols is completely unexpected.

Methane and nitrogen in Titan's atmosphere are supplied with free energy from solar ultraviolet (UV) radiation and energetic particles in Saturn's magnetosphere. These circumstances make Titan, a prolific source of complex organic compounds, unparalleled in the solar system. Hydrocarbon chemistry is further enhanced by the escape of hydrogen from the exosphere, which accelerates the conversion of methane to unsaturated hydrocarbon-nitrile species by circumventing the buildup of molecular hydrogen, thus promoting unsaturated hydrocarbon formation (*1*, *2*). Sagan and Khare (*3*) have suggested that the penultimate result of the formation of these large compounds is the generation of hydrocarbon-nitrile aerosols (tholins) thought to populate haze layers in Titan's stratosphere (*4*, *5*). Similar organic chemistry occurs during soot formation in Earth's troposphere (*6*–*8*) and may have taken place in the

---

[1] Space Science and Engineering Division, Southwest Research Institute (SWRI), 6220 Culebra Road, San Antonio, TX 78238, USA. [2] Department of Physics and Astronomy, University of Kansas, Lawrence, KS 66045, USA. [3] Department of Space and Climate Physics, Mullard Space Science Laboratory, University College London, Holmbury St. Mary, Dorking RH5 6NT, UK. [4] Department of Physics and Astronomy, University of Texas, San Antonio, TX 78249, USA.

*To whom correspondence should be addressed. E-mail: hwaite@swri.edu (J.H.W.); bmagee@swri.edu (B.M.)